







Article

Nanoscale Interaction of Endonuclease APE1 with DNA

Sridhar Vemulapalli, Mohtadin Hashemi, Yingling Chen, Suravi Pramanik, Kishor K. Bhakat and Yuri L. Lyubchenko

Topic Collection

Feature Papers in Molecular Nanoscience

Edited by

Prof. Dr. Yuri Lyubchenko







MDPI

rticle

Nanoscale Interaction of Endonuclease PE1 with DN

Sridhar Vemulapalli ¹, Mohtadin Hashemi ^{1,2}, Yingling Chen ³, Suravi Pramanik ³, Kishor K. Bhakat ^{3,*} and Yuri L. Lyubchenko ^{1,*}

- Department of Pharmaceutical Sciences, University of Nebraska Medical Center, Omaha, NE 68198-6025, US ; sridhar.vemulapalli@unmc.edu (S.V.); hashemi@auburn.edu (M.H.)
- Department of Physics, uburn University, uburn, L 36849-5318, US
- Department of Genetics, Cell Biology and natomy, University of Nebraska Medical Center, Omaha, NE 68198-5805, US ; yingling.chen@unmc.edu (Y.C.); spramanik@tesseratx.com (S.P.)
- * Correspondence: kishor.bhakat@unmc.edu (K.K.B.); ylyubchenko@unmc.edu (Y.L.L.)

bstract: purinic/apyrimidinic endonuclease 1 (PE1) is involved in DN repair and transcriptional regulation mechanisms. This multifunctional activity of PE1 should be supported by specific structural properties of PE1 that have not yet been elucidated. Herein, we applied atomic force microscopy (FM) to characterize the interactions of PE1 with DN containing two well-separated G-rich segments. Complexes of PE1 with DN containing G-rich segments were visualized, and analysis of the complexes revealed the affinity of PE1 to G-rich DN sequences, and their yield was as high as 53%. Furthermore, PE1 is capable of binding two DN segments leading to the formation of loops in the DN – PE1 complexes. The analysis of looped PE1-DN complexes revealed that PE1 can bridge G-rich segments of DN . The yield of loops bridging two G-rich DN segments was 41%. nalysis of protein size in various complexes was performed, and these data showed that loops are formed by PE1 monomer, suggesting that PE1 has two DN binding sites. The data led us to a model for the interaction of PE1 with DN and the search for the specific sites. The implication of these new PE1 properties in organizing DN , by bringing two distant sites together, for facilitating the scanning for damage and coordinating repair and transcription is discussed.

Keywords: apurinic/apyrimidinic endonuclease 1; PE1 endonuclease; G-quadruplexes; protein–DN complexes; FM imaging; DN looping



Citation: Vemulapalli, S.; Hashemi, M.; Chen, Y.; Pramanik, S.; Bhakat, K.K.; Lyubchenko, Y.L. Nanoscale Interaction of Endonuclease PE1 with DN . Int. J. Mol. Sci. 2024, 25, 5145. https://doi.org/10.3390/ijms25105145

cademic Editors: Grzegorz Wegrzyn and Benoît Ch nais

Received: 18 March 2024 Revised: 17 pril 2024 ccepted: 6 May 2024 Published: 9 May 2024



Copyright: © 2024 by the authors. Licensee MDPI, Basel, Switzerland. This article is an open access article distributed under the terms and conditions of the Creative Commons ttribution (CC BY) license (https://creativecommons.org/licenses/by/4.0/).

1. Introduction

purinic/apyrimidinic endonuclease 1 (PE1) is a multifunctional protein involved in DN repair, specifically base excision repair (BER) and nucleotide incision repair (NIR) [1–4]. PE1 is essential for maintaining genomic stability by repairing the DN damage caused by reactive oxidation species, alkylating agents, and ionizing radiation [4–6].

PE1 cleaves abasic sites in the DN , which occur due to damage or as a repair intermediate [1,2,5,7]. In addition to its role in DN repair, PE1 interacts with transcription factors such as p53, NF- κ B, and HIF-1 α and plays a vital role in DN replication and is involved in resolving stalled replication forks by repairing the damaged DN during DN replication, repair, and recombination processes [3,5,6,8-11]. It has been reported that PE1 interacts with several key enzymes such as DN polymerase delta and stimulates the activity of flap endonuclease 1 (FEN1) [6,9,12,13].

PE1 interacts with and binds G4 structures formed by G-rich DN sequences, suggesting its role in regulating gene expression [1,2,14–16]. In addition, PE1 has been reported to regulate the stability and dynamics of G4 structures by nicking or cleaving the DN backbone at specific positions, which affects the folding and unfolding of the G4 structure [1,2,5,10]. PE1 interacts with other G4-binding proteins, such as nucleophosmin and hnRNPU, and regulates their binding to G4 structures [1,2,16–18]. PE1 interactions with G4 structures and binding proteins offer potential therapeutic targets for cancer treatment and other diseases [1–3,5,7–10,19–22].

Enrichment of PE1 in gene regulatory regions and participation in transcriptional regulation led to the hypothesis that PE1 can bring together two specific DN segments on the same DN molecules, forming a loop. DN looping is a fundamental mechanism in many processes, in particular the transcriptional initiation in both prokaryotes and eukaryotes, and brings distant sites close to the promoter region [23–27]. The formation of DN loops requires binding to two or more DN segments, with loop formation being achieved by the interaction of a single protein with two or more sites or by binding two or more DN segments through a multimer. However, there is no direct evidence of PE1-mediated DN looping.

We address these questions using FM to characterize the PE1–DN complexes directly. We have previously shown that FM is instrumental in imaging various protein–DN complexes, reviewed in [28]. Specifically, we characterized looped protein–DN complexes, such as those formed by restriction enzymes [29]. Importantly, using FM, we identified additional DN binding sites in EcoRII endonuclease, allowing the formation of double-looped complexes [30]. Herein, we applied FM to characterize the interaction of PE1 with DN using a DN substrate containing two well-separated G-rich segments. Using this approach, we demonstrate the affinity of PE1 to G-specific motifs. The formation of loops was also demonstrated, but in addition to specific loops between the G-rich segments, non-specific loops are also formed. However, no G-quadruplex structures were identified on the DN substrate alone, suggesting that their formation is not required for PE1-specific binding and that such structures can be stabilized by PE1 binding. Finally, loops are formed by the monomeric PE1 protein, suggesting that the protein has two DN binding sites.

2. Results

2.1. DN Design: Preparation of the Substrate with Two PE1 Sites

We used a 673 bp DN substrate from the human genome containing two 22 bp long G-rich motifs of the *c-MYC* gene regulatory region. G-rich segments were located at positions 123 bp and 583 bp of the DN substrate (Figure 1). The DN was selected based on the previous biochemical studies conducted to characterize the PE1 interactions [1,2]. The two G-rich sites on the DN are separated by 417 bp, which, according to our previous publications, is appropriate for the assembly and the FM visualization of the protein-mediated DN loops [29].

Typical FM images of the G-rich DN substrate are shown in Figure 1B, in which DN appears as smooth filaments. The contour length measurements are shown in Figure 1C. total of N=300 particles was analyzed, and a single peak Gaussian function approximation of the histogram gives a mean of 672 $\,$ 31 bp (SD). Similar contour length measurements of the control DN $\,$ of 612 bp with no G-rich segments are shown in Figure 1D.

2.2. PE1 Complex ssembly and Loop Size nalysis

The PE1–DN complexes were assembled at a 1:1 protein/DN ratio and prepared for FM imaging. FM images of the PE1–DN complexes are shown in Figure 2 with a few zoomed images shown in Figure 2B,C. Three different morphologies were identified: bare DN (Figure 2B(1)); DN with PE1 as bright globular features (Figure 2B(2,3)) and looped DN with PE1 as globular features (Figure 2C(1–3)). The overall yield of complexes is 53%, with the partition of looped and non-looped complexes 22% and 31%, respectively (Table 1).

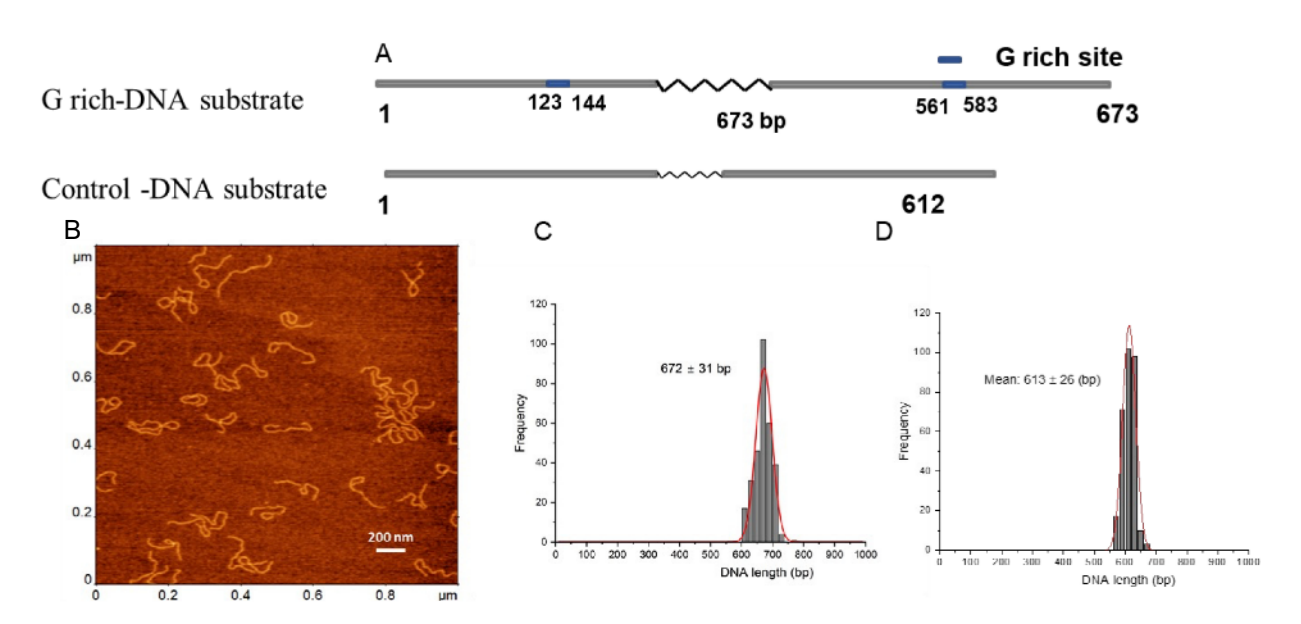


Figure 1. DN substrates, FM image, and contour length. () The schematic for the G rich-substrates (upper scheme) and the control (bottom). 22 bp G-rich motifs are located at 123–144 bp and at 561–583 bp and are shown in blue. The non-G-rich DN substrate with 612 bp in length was used as a control. (**B**). typical 1×1 m FM scan of G-rich DN substrate (**C**,**D**) are histograms for the contour length measurements for G-rich DN substrate and the control, respectively. Each distribution is approximated with single Gaussians built with a bin size of 20 bp. The contour length values in base pairs and standard deviations are indicated for each histogram.

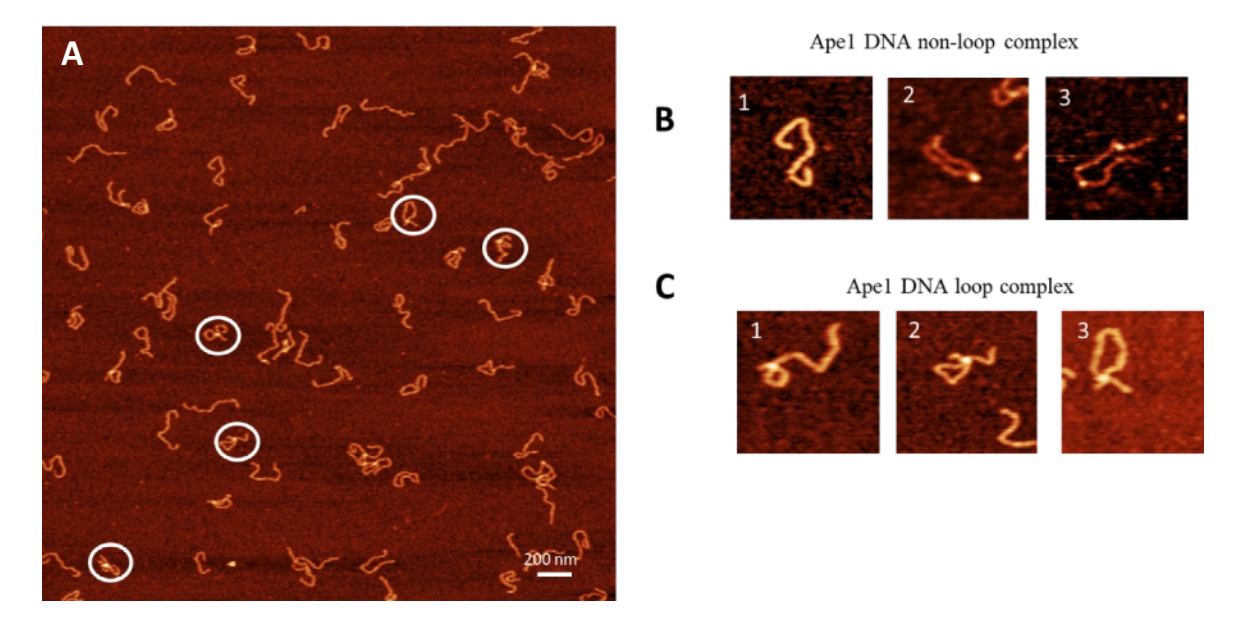


Figure 2. FM image of complexes of PE1 with G-rich DN complexes (1:1). () The FM image with looped complexes of PE1-G-rich-DN . Zoomed images of complexes circled in () are indicated in (**B,C**). (**B**) set of images with no PE1 bound (frame 1) and non-looped complexes with one PE1 bound (frame 2) and two PE1 bound (frame 3). (**C**) set of three looped complexes with different sizes of loops.

Substrate	N = 500	PE1-DN Complex (Non-Looped Complexes)	PE1-DN Complex (Complexes with Loops)
G rich-DN	Yield [%].	31%	22%
Non-G rich DN	Yield [%].	15%	4%

 $\textbf{Table 1.} \ \ \textbf{The yield of} \quad \textbf{PE1-DN} \quad \textbf{complexes formed on G-rich and non-G-rich substrates}.$

Similar experiments were performed for the control DN substrate containing no G-rich sequences. The FM images are shown in Figure 3 . Similar to the G-rich DN substrate, three different morphologies were observed with selected zoomed images shown in Figure 3B,C. These are free DN (Figure 3B(1)), DN with bright features (Figure 3B(2,3)), and looped complexes (Figure 3C(1–3)). The overall yield of complexes is 19%, with the yield of looped complexes being 4% (Table 1).

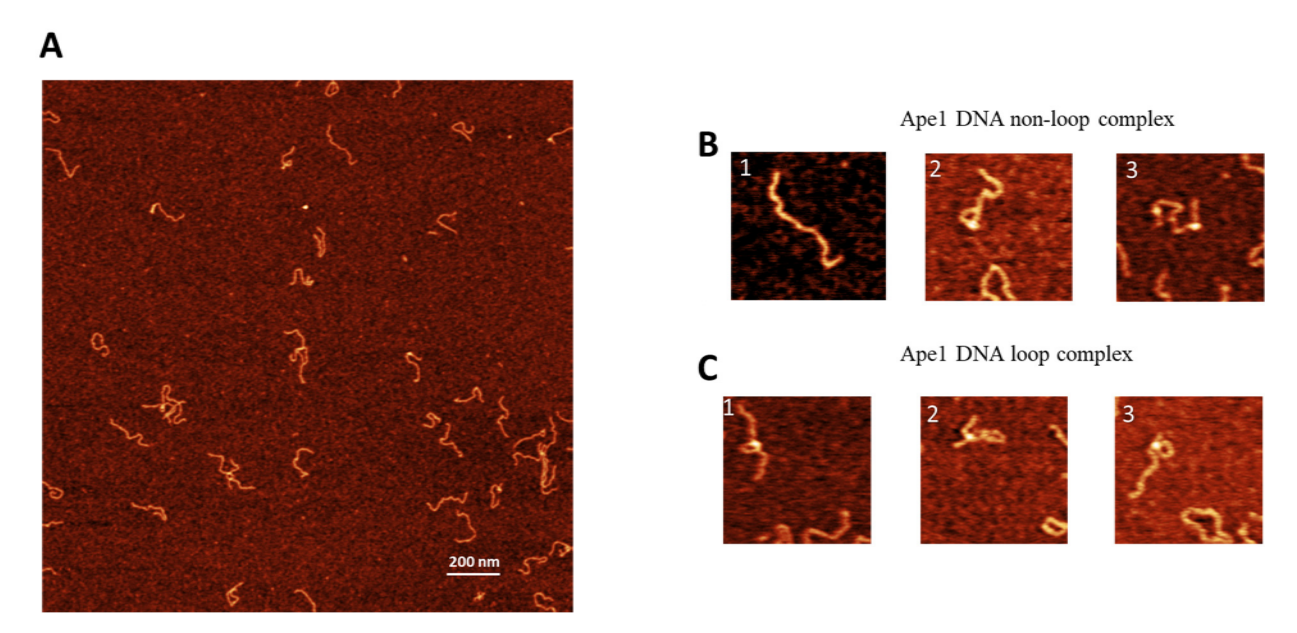


Figure 3. FM image of complexes of PE1 with non-G-rich DN complexes (control substrate). () typical FM scan with 3×3 in size. shows the FM image with looped complexes of PE1–non-G rich-DN . (**B**) and (**C**) show a few examples of complexes with linear morphology and looped DN complexes, respectively.

2.3. FM Data nalysis: Positioning of PE1 on DN

Given the relative symmetry in the position of G-rich segments on the DN $\,$, relative to the DN $\,$ ends (123–144 bp and 561–583 bp), we mapped the positions of $\,$ PE1 on the G-rich DN $\,$ by measuring the length of the distance between the bright features and closest DN $\,$ end (Figure 4 $\,$). The measurements were made for 300 complexes and the results are shown as a histogram in Figure 4B. Green vertical lines indicate positions of the G-rich motifs in the DN $\,$ molecule. Positions of $\,$ PE1 within the range of the green lines are considered as specific interactions of $\,$ PE1 with DN $\,$.

similar analysis was carried out for complexes of $\,$ PE1 with the control DN substrate. The histogram of the $\,$ PE1 position measured from the end of the DN $\,$ molecule is shown in Figure S4 $\,$.

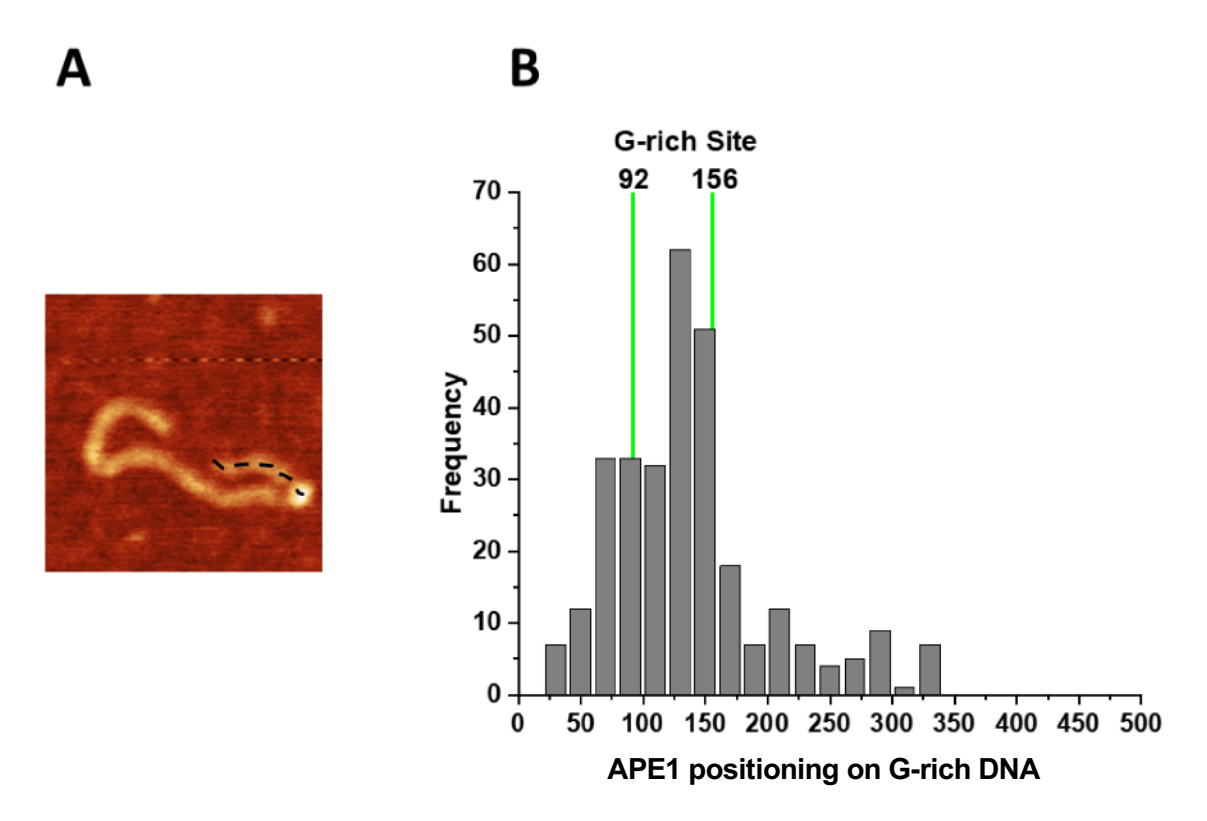


Figure 4. Mapping of the PE1 positions on the G-rich-DN substrate. () FM image of PE1–G rich-DN complex. The dotted line illustrates the contour length of the short arm measured from the DN end to the center of the protein. (**B**) The histogram of PE1 mapping performed over 300 molecules. Vertical green lines correspond to the range of distances from both DN ends to G-rich motifs, which includes the 22 bp size of the motifs. Locations of PE1 within the 92–156 bp range correspond to the specific binding of the protein.

2.4. FM Data nalysis: Sizes of DN Loops

For looped PE1–DN complexes, two parameters were measured: the loop sizes and the lengths of the flanks. The results are assembled in Figure 5. The loop sizes are shown in Figure 5 and have a narrow distribution around 410 bp with a spread between \sim 350 bp and \sim 450 bp, which, when taking into account the 22 bp size of the G-rich motifs, corresponds to the assembly of complexes between the G-rich sites. Data beyond this size correspond to the formation of non-specific loops.

The results for measurements of short and long flanks are shown in Figure 5C,D, respectively. The short flank length distribution is narrow and spans over the range of 60–150 bp, which, due to the 22 bp length of the G-rich sites, covers the expected position for binding PE1 to one or the other G-rich sites. On the other hand, the distribution of the lengths of the long arm is broad. In addition to the range corresponding to PE1 binding to one or the other G-rich sites (vertical lines), events corresponding to the assembly of loops with PE1 binding to non-specific sites are also present.

The yield of looped complexes for the control DN substrate was 4%, which is ~1/6 compared to complexes assembled on a G-rich DN substrate (see Table 1). The control substrate's loop sizes were analyzed, and the data are shown in Figure S4B. The distribution was broad and flat, with no preferential loop size identifiable, indicative of a random distribution, which is corroborated by simulated distribution for non-specific looping (Figure S5).

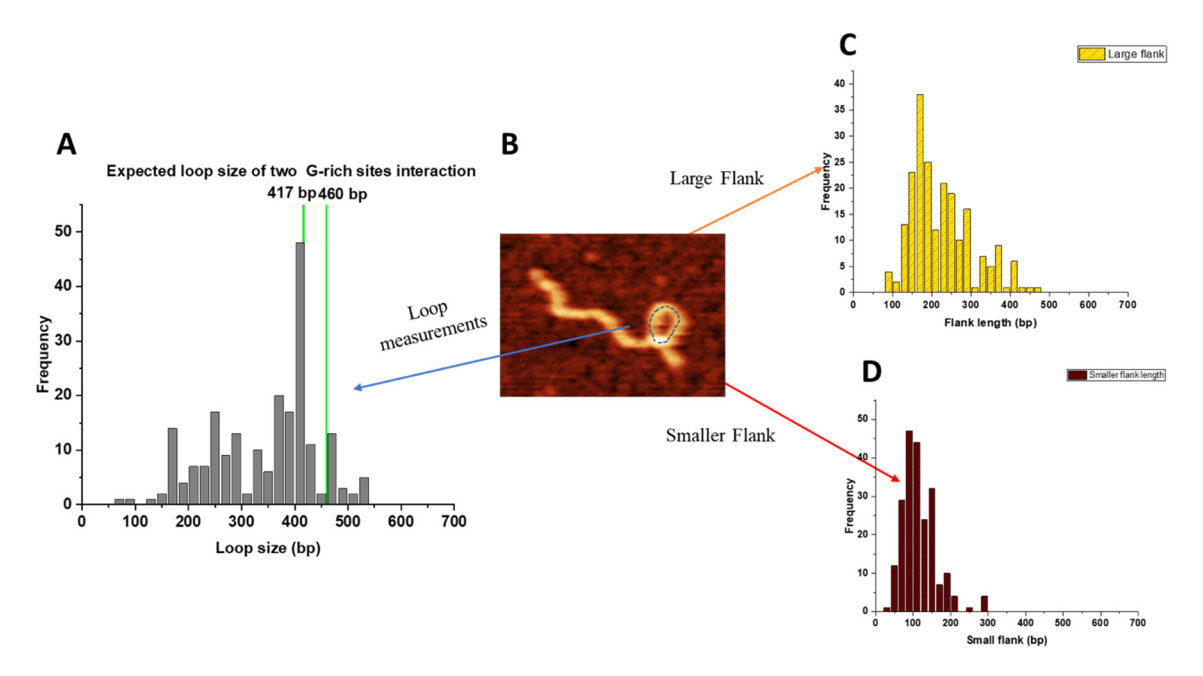


Figure 5. Looped complexes formed by PE1 on the G-rich DN substrate. () The histogram for the loop sizes obtained for 200 looped complexes. Vertical green lines indicate the sizes of loops formed by bridging of two G-rich motifs, which includes their sizes. (**B**) FM image showing the looped complex. The loop is indicated using a dotted line. (**C**) The histogram of the lengths of the long arms. (**D**) The histogram of the lengths of short arms.

2.5. Looped Structures re Formed by Monomeric PE1

FM captures the 3D shape of molecules and allows evaluation of their sizes. We used the height and volume measurements to estimate the molecular weights of proteins complexed with DN [31,32]. This information clarifies whether PE1 monomers, dimers, or larger oligomers are responsible for assembling loops. The two different pathways impose certain conditions; in the case of the dimeric stoichiometry in the looped complexes, each monomer should bind to DN first, and then the loop is formed via protein–protein interactions. If the monomeric PE1 makes loops, the protein should have two DN binding sites.

First, we measured the PE1 protein height in non-looped complexes with DN on the G-rich substrate (Figure 6) and obtained the height histogram (Figure 6B), which approximated with a Gaussian shows a peak at 1.2 0.2 nm. The corresponding volume of the protein displayed a Gaussian distribution with a mean value of 125 45 nm³ (Figure 6C). Next, we measured the same parameters for PE1 in looped complexes (Figure 6D). The height histogram for the protein in looped complexes was approximated with a Gaussian distribution and yielded a mean value of 1.1 0.13 nm (Figure 6E). Similarly, the volume of the protein displayed a Gaussian distribution centered around 130 51 nm³ (Figure 6F).

s a control, we measured the height and volume of the PE1 protein in complexes with the control DN substrate. The height of the protein in this complex showed a Gaussian distribution with a mean value of the height of 1.1 0.13 nm, as shown in Figure 7. The volume of the protein exhibited a Gaussian distribution centered around 114 19 nm³ (Figure 7B). The height and volume of the PE1 protein in looped complexes with the control DN produced values 1.07 0.12 nm and 117 14 nm³ (Figure 7C,D), which are indistinguishable from those obtained for the G-rich DN substrate.

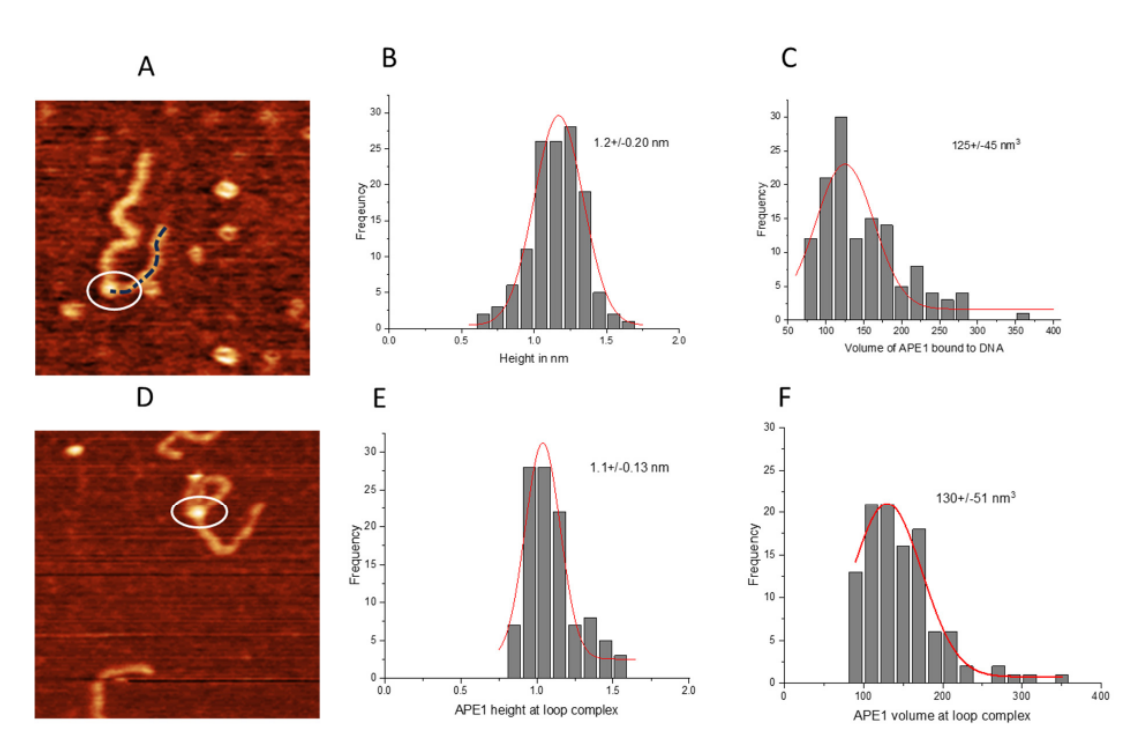


Figure 6. The height and volume analysis of the PE1 on G-rich DN with the non-looped and looped complexes. () FM image of the PE1 protein positioned on linear DN . Circle highlights the PE1 protein, while dotted line illustrates the short DN flank. (**B**) Histograms for height values of the PE1 protein approximated with a Gaussian distribution (1.2 0.20 nm). (**C**) The histogram of the volume measurements data approximated with a Gaussian distribution (125 45 nm³). (**D**) FM image of looped complexes of PE1 protein (circled). (**E**) The histogram for the protein height approximated with a Gaussian distribution (1.1 0.13 nm). (**F**) The histogram for the protein volume approximated with a Gaussian distribution (130 51 nm³).

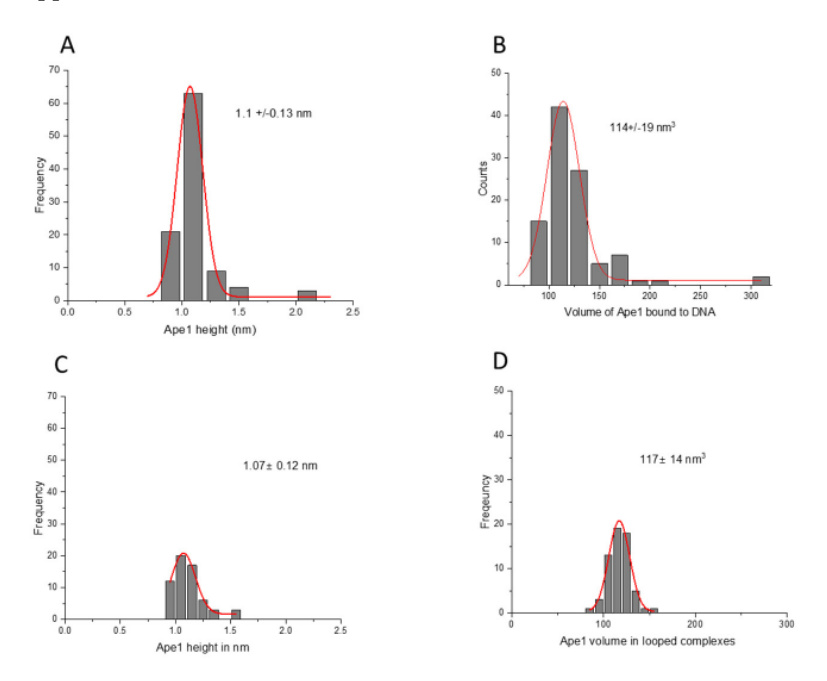


Figure 7. Height and volume measurements for complexes of the PE1 on control DN substrate with non-looped and looped complexes. () and (**B**) are the histograms for the protein heights and volume, respectively, for non-looped complexes. (**C**) and (**D**) are the histograms for the height and volume of PE1, respectively. Each histogram is approximated by single Gaussians with parameters indicated in the plots.

Height measurements of free $\,$ PE1 produced the value 0.53 $\,$ 0.14 nm (Figure 8B), which, combined with the DN $\,$ height ~0.5 nm, produces the height value ~1.1 nm (Figure 8C) for the protein bound to DN $\,$. This value is close to the height values measured for protein bound to DN $\,$, suggesting that protein binding to DN $\,$ is not accompanied by its oligomerization.

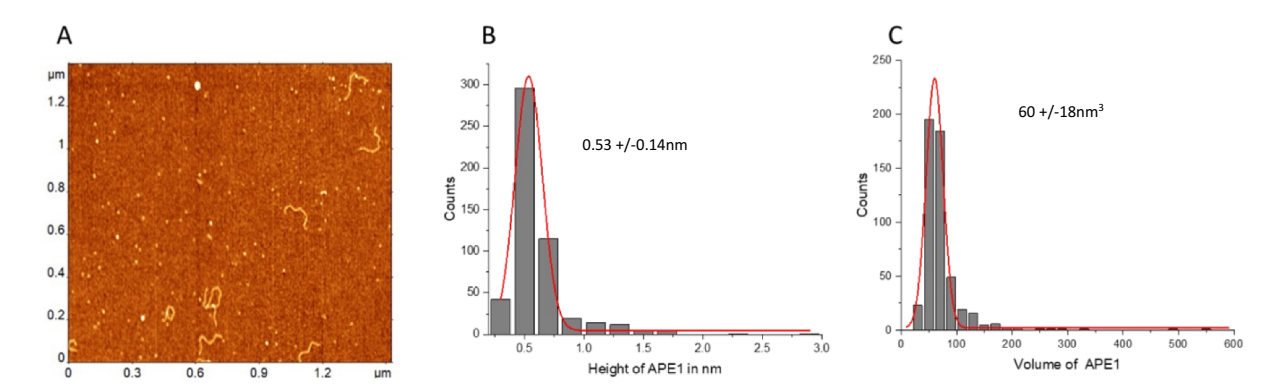


Figure 8. Height and volume measurements of the free PE1 protein. () FM images of the free protein with added DN as a reference. (**B**,**C**) are the histograms for the height and volume values built for 100 measurements. The histograms are approximated with Gaussians with parameters indicated in the plots.

These findings suggest that the monomeric form or single PE1 is involved in bridging two distant sites, suggesting that PE1 has two DN binding segments and both are involved in the DN looping.

3. Discussion

 $\,$ FM studies clarified several novel features involved in the interaction of $\,$ PE1 with DN $\,$.

The binding of PE1 to the G-rich motifs was previously shown using various indirect studies; here, visualization with FM directly evaluated the specificity of PE1 binding to G-rich segments. In addition, analysis of FM data revealed that PE1 is capable of binding to non-G DN as well, with the yield of such complexes being approximately two-fold lower than the formation of specific PE1–G complexes (Figure S4).

Studies have shown that quadruplex formation and stability can depend on the ionic species present [33–36]. Herein, experiments were performed in the presence of K⁺ ions, which have been shown to be favorable for the formation of quadruplex structures [35–37]. However, FM images of only DN (Figure 1) demonstrated that the G-rich DN molecules are smooth and indistinguishable from the control, without G-rich segments, in contrast to G quadruplexes routinely visualized with FM [38,39]. Note that in vitro colocalization studies showed PE1 localization to quadruplex sites [1,2]. These studies lead the authors to hypothesize that, in cells, it is not the G-rich dsDN sequence per se but the formation of quadruplex DN secondary structure that recruits PE1 to the promoter-enhancer regions to regulate repair and transcription. However, studies in this paper demonstrate that no quadruplexes are formed stably in the G-rich DN substrate. the same time, it has been reported that PE1 stabilizes quadruplex structures [1]. It is not possible to detect DN morphology with PE1 bound to the G-rich segment, as the protein will cover the bound DN segment. However, a change in DN morphology should translate to a change in protein–DN complex height and volume. Neither height nor volume of PE1 (Figures 6 and 7), bound to DN or participating in loop formation, were significantly different when comparing PE1 interacting with the G-rich DN construct versus the control DN construct without G-rich segments.

Looping was another putative function of PE1 that we provide evidence for here. PE1 is capable of binding two sites on the same DN molecule, leading to the formation of looped DN structures. nalysis of FM data showed that loops of different sizes are formed, and loops corresponding to the bridging of two G-rich segments were also visualized. The yield of such G-specific loops is close to the yield of non-specific loops, which is in line with the findings regarding the binding of PE1 to G-rich and non-specific linear DN . However, additional quantitative analysis of looped complexes revealed an interesting assembly feature. s demonstrated in Figure 5, looped complexes in the vast majority of cases have short flanks with the length corresponding to the position of G-rich sites. In other words, PE1 in the loops binds to one G-rich site and one other site, which can be another G-rich site or any non-G-rich segment.

The FM images allowed us to elucidate the PE1 stoichiometry in the looped complexes. We determined the stoichiometry of PE1 in looped complexes by performing measurements of the protein sizes. The data shown in Figures 2–4 demonstrate that looped complexes are formed by monomeric PE1 rather than its dimer. PE1 multimers were expected based on previous studies by Kladova et al., which show that PE1 multimers are integral for their function in the base excision repair process [40]. Bridging of two DN binding sites is possible if the proteins have multiple DN binding sites [30]. The binding of two DN segments by the monomeric PE1 suggests the protein has two binding sites. s we discussed above, looped complexes on the G-rich DN substrate almost always have PE1 bound to one G-rich segment. This finding leads to the hypothesis that one DN binding site of PE1 has a strong specificity to G-rich sequences, and the other site is more promiscuous.

We recently proposed the model for the site search process during DN looping based on studies of the highly sequence-specific restriction enzyme SfiI [29]. ccording to this model, during the search process, the protein initially binds to a specific site, grabs any non-specific site, and threads DN in search of another specific site. In the framework of this model, we hypothesize that PE1 binds to the G-rich region on DN at its specific site and searches DN by using its less specific site. Note that such a mechanism has recently been proposed for the DN looping for cohesin [41]. PE1-mediated DN looping for bringing two distant sites together may facilitate damage search in the transcriptional regulatory regions, coordinating repair and long-range promoter—enhancer interaction for repair and transcription.

4. Materials and Methods

4.1. PE1-Protein

The full-length PE1 coding sequence was inserted in the pET15b vector (Novagen, Madison, WI, US) at NdeI/Xho I sites for expression of PE1 in the E. coli Rosetta 2 strain (Novagen). The DN sequence of the PE1 was confirmed by the UNMC genomic PE1 protein was purified as previously described [42] with slight modifications. fter transforming with the pET15b-based PE1 expression plasmid, E. coli were grown to 0.6 OD at 600 nm. PE1 expression was then induced with 0.5 mM isopropyl-β-Dthiogalactopyranoside (IPTG) at 18 °C for 16 h. The cells were then suspended in a buffer containing 20 mM Tris (pH 8.0) and 0.5 M NaCl, sonicated, and centrifuged. The supernatant was loaded onto the Ni-NT (Qiagen, Germantown, MD, US) column (3 mL), run, and then eluted with buffer containing 200 mM imidazole. The eluate was dialyzed against 20 mM Tris-Cl (pH 8.0), 100 mM NaCl, 1 mM EDT , 1 mM dithiothreitol (DTT), and 10% glycerol. The poly His-tag in the protein was cleaved by overnight incubation at 4 °C with thrombin. The PE1 was finally purified by FPLC using an SP-Sepharose column (LCC-500 PLUS; Pharmacia, Chicago, IL, US), and the final preparation was dialyzed against 20 mM Tris (pH 8.0), 300 mM NaCl, 0.1 mM EDT , 1 mM DTT, 50% glycerol, and stored at -20 °C.

4.2. DN Substrates

673 bp DN segment of the c-MYC gene promoter (-25 to -648 bp with respect to the transcription start site) was amplified by PCR and formed the DN substrate containing two G-rich motifs (Figure 1). For the PCR reaction, 100 ng of human genome DN and PfuUltra High-Fidelity DN polymerase (#600380) were used with the primers: Forward primer: GGGTTTG G GGG GC G; Reverse primer: CTCGGGTGTTG-T GTTCC G. Similarly, DN without G-rich motifs with a length of 612 bp, as shown in (Figure 1), was obtained by performing PCR of the plasmid.

Both DN substrates were gel-purified as described [29]. Briefly, the PCR product was run on a 1% agarose gel. The product bands corresponding to the expected length of the DN were excised, and DN was extracted and purified using the Qiagen DN gel extraction kit (Qiagen Inc., Valencia, C , US). The final DN concentration was determined by absorbance at 260 nm using a NanoDrop spectrophotometer (NanoDrop Technologies, Wilmington, DE, US).

4.3. PE1-DN Synaptosome ssembly

DN was mixed with PE1 enzyme at the molar ratio 1:1 in 50 mM Tris-HCl buffer containing 50 mM KCl, 2 mM MgCl $_2$ with a total volume of 10 L, and with the final concentrations of DN and PE1 at 1 nM. reaction mixture for PE1-DN assembly consisted of a final volume of 10 L with 7 L of 1X buffer [50 mM Tris HCl (pH 7.5), 50 mM KCl, 2 mM MgCl $_2$, 0.1 mM EDT], 1 L of 10 mM DTT, 1 L of DN , and 1 L of protein. The reaction mixture was incubated for 15 min at room temperature.

4.4. tomic Force Microscopy

The PE1–DN complexes were deposited on functionalized mica and functionalized with 1-(3-aminopropyl)-silatrane, as described previously [29]. Briefly, 3–4 L of PE1-DN reaction mixture was deposited on the functionalized mica surface, incubated for 2 min, rinsed with deionized water, dried with argon, and stored under vacuum until imaged.

typical FM image scanned 3×3 m area with 1536 pixels/line under ambient conditions. Imaging was performed with a MultiMode 8 FM system using TESP probes (Bruker Nano, Camarillo, C , US).

4.5. Data nalysis

The contour length of the bare DN , the PE1–DN complexes, and the looped PE1–DN complexes were measured using FemtoScan software (version 2.4.10, dvanced Technologies Center, Moscow, Russia) as described previously [29], which allows reliable tracing of DN , as shown in Figure S1. Figures S2 and S3 illustrate the measurements of the protein position and loop size, respectively.

The yield of complexes was calculated by comparing the number of free DN $\,$ molecules with DN $\,$ molecules with PE1. The yield of looped complexes was also calculated based on the comparison with free DN $\,$, and not the $\,$ PE1–DN $\,$ complexes, and provides an absolute yield percentage.

4.6. Height and Volume of PE1

Grain analysis (FemtoScan software) was performed to measure the height and volume of the free PE1, PE1 complexed with DN , and PE1 in looped complexes.

5. Conclusions

Our data shed light on whether PE1 recognizes G-rich regions [43]. FM images of the DN templates (Figure 1) demonstrate that the G-rich DN segments were smooth and indistinguishable from the control. In contrast, G quadruplexes were considerably wider than the DN duplex and could be visualized routinely with FM [38,39]. Thus, no quadruplexes were formed stably in the G-rich DN substrate. t the same time, the

specificity of PE1 to G-rich sequences was shown, with approximately two-fold yield compared to non-G construct, suggesting that PE1 can bind to G-rich sequences without converting them into G quartet [14,44]. Our studies demonstrate that monomeric PE1 is capable of bridging two distant DN segments, suggesting that PE1 should have two DN binding sites. We hypothesize that one of them is specific for binding to G-rich sequences, and based on this hypothesis, we proposed the site search mechanism for PE1.

Supplementary Materials: The following supporting information can be downloaded at: https://www.mdpi.com/article/10.3390/ijms25105145/s1, detailed description of the DN contour length, PE-1 positioning, and loop complexes measurements was provided.

uthor Contributions: Y.L.L. designed and supervised the project. K.K.B. initiated the project. S.V. and M.H. designed and performed the experiments and data analysis. Y.C. and S.P. prepared PE1 and DN samples. Il authors contributed to writing the manuscript. Il authors have read and agreed to the published version of the manuscript.

Funding: This work was supported by NSF grant MCB 1941049 to Y.L.L.

Data vailability Statement: Il data are included in the manuscript and the Supplementary Materials.

cknowledgments: We thank L. Shlyakhtenko (the University of Nebraska Medical Center) for valuable insights, Shaun Filliaux for proofreading the manuscript, and all Y.L.L. lab members for fruitful discussions of the results.

Conflicts of Interest: The authors declare no competing financial interests.

References

- 1. Roychoudhury, S.; Pramanik, S.; Harris, H.L.; Tarpley, M.; Sarkar, .; Spagnol, G.; Sorgen, P.L.; Chowdhury, D.; Band, V.; Klinkebiel, D.; et al. Endogenous oxidized DN bases and PE1 regulate the formation of G-quadruplex structures in the genome. *Proc. Natl.* cad. Sci. US 2020, 117, 11409–11420. [CrossRef] [PubMed]
- 2. Pramanik, S.; Chen, Y.; Song, H.; Khutsishvili, I.; Marky, L.; Ray, S.; Natarajan, .; Singh, P.K.; Bhakat, K.K. The human P-endonuclease 1 (PE1) is a DN G-quadruplex structure binding protein and regulatesKR Sexpression in pancreatic ductal adenocarcinoma cells. *Nucleic cids Res.* **2022**, *50*, 3394–3412. [CrossRef] [PubMed]
- 3. Li, M.; Wilson, D.M. Human purinic/ pyrimidinic Endonuclease 1. *ntioxid. Redox Signal.* **2014**, 20, 678–707. [CrossRef] [PubMed]
- 4. Bhakat, K.K.; Izumi, T.; Yang, S.; Hazra, T.K.; Mitra, S. Role of acetylated human P-endonuclease (PE1/Ref-1) in regulation of the parathyroid hormone gene. *EMBO J.* **2003**, 22, 6299–6309. [CrossRef] [PubMed]
- 5. Thakur, S.; Sarkar, B.; Cholia, R.P.; Gautam, N.; Dhiman, M.; Mantha, .K. PE1/Ref-1 as an emerging therapeutic target for various human diseases: Phytochemical modulation of its functions. *Exp. Mol. Med.* **2014**, *46*, e106. [CrossRef]
- 6. Tell, G.; Quadrifoglio, F.; Tiribelli, C.; Kelley, M.R. The Many Functions of PE1/Ref-1: Not Only a DN Repair Enzyme. *ntioxid. Redox Signal.* **2009**, *11*, 601–619. [CrossRef] [PubMed]
- 7. Thakur, S.; Dhiman, M.; Tell, G.; Mantha, .K. review on protein–protein interaction network of PE1/Ref-1 and its associated biological functions. *Cell Biochem. Funct.* **2015**, *33*, 101–112. [CrossRef] [PubMed]
- 8. Evans, .R.; Limp-Foster, M.; Kelley, M.R. Going PE over ref-1. Mutat. Res. Repair 2000, 461, 83–108. [CrossRef]
- 9. Frossi, B.; ntoniali, G.; Yu, K.; khtar, N.; Kaplan, M.H.; Kelley, M.R.; Tell, G.; Pucillo, C.E. Endonuclease and redox activities of human apurinic/apyrimidinic endonuclease 1 have distinctive and essential functions in Ig class switch recombination. *J. Biol. Chem.* **2019**, 294, 5198–5207. [CrossRef]
- 10. Oliveira, T.T.; Coutinho, L.G.; de Oliveira, L.O. .; Timoteo, .R.d.S.; Farias, G.C.; gnez-Lima, L.F. PE1/Ref-1 Role in Inflammation and Immune Response. *Front. Immunol.* **2022**, *13*, 793096. [CrossRef]
- 11. Hoitsma, N.M.; Norris, J.; Khoang, T.H.; Kaushik, V.; Chadda, R.; ntony, E.; Hedglin, M.; Freudenthal, B.D. Mechanistic insight into P-endonuclease 1 cleavage of abasic sites at stalled replication fork mimics. *Nucleic cids Res.* **2023**, *51*, 6738–6753. [CrossRef]
- 12. Jaiswal, S.; Williamson, E.; Srinivasan, G.; Kong, K.; Lomelino, C.L.; McKenna, R.; Walter, C.; Sung, P.; Narayan, S.; Hromas, R. The splicing component ISY1 regulates PE1 in base excision repair. *DN Repair* **2019**, *86*, 102769. [CrossRef] [PubMed]
- 13. Park, S.H.; Kim, Y.; Ra, J.S.; Wie, M.W.; Kang, M.-S.; Kang, S.; Myung, K.; Lee, K.-Y. Timely termination of repair DN synthesis by T D5 is important in oxidative DN damage-induced single-strand break repair. *Nucleic cids Res.* **2021**, *49*, 11746–11764. [CrossRef] [PubMed]
- 14. Fleming, .M.; Manage, S. .H.; Burrows, C.J. Binding of P Endonuclease-1 to G-Quadruplex DN Depends on the N-Terminal Domain, Mg²⁺, and Ionic Strength. *CS Bio Med Chem u* **2021**, *1*, 44–56. [CrossRef]

15. Dumas, L.; Herviou, P.; Dassi, E.; Cammas, .; Millevoi, S. G-Quadruplexes in RN Biology: Recent dvances and Future Directions. *Trends Biochem. Sci.* **2020**, *46*, 270–283. [CrossRef]

- 16. Pavlova, .V.; Kubareva, E. .; Monakhova, M.V.; Zvereva, M.I.; Dolinnaya, N.G. Impact of G-Quadruplexes on the Regulation of Genome Integrity, DN Damage and Repair. *Biomolecules* **2021**, *11*, 1284. [CrossRef] [PubMed]
- 17. Miclot, T.; Corbier, C.; Terenzi, .; Hognon, C.; Grandemange, S.; Barone, G.; Monari, . Forever Young: Structural Stability of Telomeric Guanine Quadruplexes in the Presence of Oxidative DN Lesions. *Chem. Eur. J.* **2021**, 27, 8865–8874. [CrossRef]
- 18. Vascotto, C.; Fantini, D.; Romanello, M.; Cesaratto, L.; Deganuto, M.; Leonardi, ..; Radicella, J.P.; Kelley, M.R.; D' mbrosio, C.; Scaloni, ..; et al. PE1/Ref-1 Interacts with NPM1 within Nucleoli and Plays a Role in the rRN Quality Control Process. *Mol. Cell. Biol.* 2009, 29, 1834–1854. [CrossRef]
- 19. Curtis, C.D.; Thorngren, D.L.; Ziegler, Y.S.; Sarkeshik, .; Yates, J.R.; Nardulli, .M. purinic/ pyrimidinic Endonuclease 1 lters Estrogen Receptor ctivity and Estrogen-Responsive Gene Expression. *Mol. Endocrinol.* **2009**, 23, 1346–1359. [CrossRef]
- Lee, Y.R.; Kim, K.M.; Jeon, B.H.; Choi, S. Extracellularly secreted PE1/Ref-1 triggers apoptosis in triple-negative breast cancer cells via R GE binding, which is mediated through acetylation. Oncotarget 2015, 6, 23383–23398. [CrossRef]
- 21. Woo, J.; Park, H.; Sung, S.H.; Moon, B.-I.; Suh, H.; Lim, W. Prognostic Value of Human purinic/ pyrimidinic Endonuclease 1 (PE1) Expression in Breast Cancer. *PLoS ONE* **2014**, *9*, e99528. [CrossRef]
- 22. Bhakat, K.K.; Mantha, .K.; Mitra, S. Transcriptional Regulatory Functions of Mammalian P-Endonuclease (PE1/Ref-1), an Essential Multifunctional Protein. *ntioxid. Redox Signal.* **2009**, *11*, 621–637. [CrossRef]
- 23. Matthews, K.S. DN looping. Microbiol. Rev. 1992, 56, 123–136. [CrossRef] [PubMed]
- 24. Cournac, .; Plumbridge, J. DN Looping in Prokaryotes: Experimental and Theoretical pproaches. *J. Bacteriol.* **2013**, 195, 1109–1119. [CrossRef] [PubMed]
- 25. Perez, P.J.; Clauvelin, N.; Grosner, M. .; Colasanti, .V.; Olson, W.K. What Controls DN Looping? *Int. J. Mol. Sci.* 2014, 15, 15090–15108. [CrossRef] [PubMed]
- 26. Fogg, J.M.; Judge, .K.; Stricker, E.; Chan, H.L.; Zechiedrich, L. Supercoiling and looping promote DN base accessibility and coordination among distant sites. *Nat. Commun.* **2021**, *12*, 5683. [CrossRef] [PubMed]
- 27. Vilar, J.M.; Saiz, L. DN looping in gene regulation: From the assembly of macromolecular complexes to the control of transcriptional noise. *Curr. Opin. Genet. Dev.* **2005**, *15*, 136–144. [CrossRef] [PubMed]
- 28. Lyubchenko, Y.L. Direct FM visualization of the nanoscale dynamics of biomolecular complexes. *J. Phys. D ppl. Phys.* **2018**, *51*, 403001. [CrossRef] [PubMed]
- 29. Vemulapalli, S.; Hashemi, M.; Lyubchenko, Y.L. Site-Search Process for Synaptic Protein-DN Complexes. *Int. J. Mol. Sci.* **2021**, 23, 212. [CrossRef]
- 30. Shlyakhtenko, L.S.; Gilmore, J.; Portillo, .; Tamulaitis, G.; Siksnys, V.; Lyubchenko, Y.L. Direct visualization of the EcoRII DN triple synaptic complex by atomic force microscopy. *Biochemistry* **2007**, *46*, 11128–11136. [CrossRef]
- 31. Lushnikov, .Y.; Potaman, V.N.; Oussatcheva, E. .; Sinden, R.R.; Lyubchenko, Y.L. DN Strand rrangement within the SfiI-DN Complex: tomic Force Microscopy nalysis. *Biochemistry* **2006**, *45*, 152–158. [CrossRef] [PubMed]
- 32. Pan, Y.; Shlyakhtenko, L.S.; Lyubchenko, Y.L. High-speed atomic force microscopy directly visualizes conformational dynamics of the HIV Vif protein in complex with three host proteins. *J. Biol. Chem.* **2020**, 295, 11995–12001. [CrossRef] [PubMed]
- 33. Li, X.; Sánchez-Ferrer, .; Bagnani, M.; damcik, J.; zzari, P.; Hao, J.; Song, .; Liu, H.; Mezzenga, R. Metal ions confinement defines the architecture of G-quartet, G-quadruplex fibrils and their assembly into nematic tactoids. *Proc. Natl. cad. Sci. US* 2020, 117, 9832–9839. [CrossRef]
- 34. Zhou, W.; Lai, R.; Cheng, Y.; Bao, Y.; Miao, W.; Cao, X.; Jia, G.; Li, G.; Li, C. Insights into How NH₄⁺ Ions Enhance the ctivity of Dimeric G-Quadruplex/Hemin DN zyme. *CS Catal.* **2023**, *13*, 4330–4338. [CrossRef]
- 35. Tong, X.; Ga, L.; Eerdun, C.; Zhao, R.; i, J. Simple Monovalent Metal Ion Logical Order to Regulate the Secondary Conformation of G-Quadruplex. *CS Omega* **2022**, *7*, 39224–39233. [CrossRef]
- 36. Schultze, P.; Hud, N.V.; Smith, F.W.; Feigon, J. The effect of sodium, potassium and ammonium ions on the conformation of the dimeric quadruplex formed by the Oxytricha nova telomere repeat oligonucleotide d(G4T4G4). *Nucleic cids Res.* 1999, 27, 3018–3028. [CrossRef] [PubMed]
- 37. Marathias, V.M.; Bolton, P.H. Determinants of DN Quadruplex Structural Type: Sequence and Potassium Binding. *Biochemistry* **1999**, *38*, 4355–4364. [CrossRef] [PubMed]
- 38. Neaves, K.J.; Huppert, J.L.; Henderson, R.M.; Edwardson, J.M. Direct visualization of G-quadruplexes in DN using atomic force microscopy. *Nucleic cids Res.* **2009**, *37*, 6269–6275. [CrossRef] [PubMed]
- 39. bdelhady, H.G.; llen, S.; Davies, M.C.; Roberts, C.J.; Tendler, S.J.B.; Williams, P.M. Direct real-time molecular scale visualisation of the degradation of condensed DN complexes exposed to DNase I. *Nucleic cids Res.* **2003**, *31*, 4001–4005. [CrossRef]
- 40. Kladova, O. .; Bazlekowa-Karaban, M.; Baconnais, S.; Pi trement, O.; Ishchenko, . .; Matkarimov, B.T.; Iakovlev, D. .; Vasenko, .; Fedorova, O.S.; Le Cam, E.; et al. The role of the N-terminal domain of human apurinic/apyrimidinic endonuclease 1, PE1, in DN glycosylase stimulation. DN Repair 2018, 64, 10–25. [CrossRef]
- 41. Pugacheva, E.M.; Kubo, N.; Loukinov, D.; Tajmul, M.; Kang, S.; Kovalchuk, .L.; Strunnikov, .V.; Zentner, G.E.; Ren, B.; Lobanenkov, V.V. CTCF mediates chromatin looping via N-terminal domain-dependent cohesin retention. *Proc. Natl. cad. Sci. US* 2020, 117, 2020–2031. [CrossRef] [PubMed]

42. Mantha, .K.; Oezguen, N.; Bhakat, K.K.; Izumi, T.; Braun, W.; Mitra, S. Unusual Role of a Cysteine Residue in Substrate Binding and ctivity of Human P-Endonuclease 1. J. Mol. Biol. 2008, 379, 28–37. [CrossRef] [PubMed]

- 43. Manage, S. .H.; Zhu, J.; Fleming, .M.; Burrows, C.J. Promoters vs. telomeres: P-endonuclease 1 interactions with abasic sites in G-quadruplex folds depend on topology. *RSC Chem. Biol.* **2023**, *4*, 261–270. [CrossRef]
- 44. Reshetnikov, R.V.; Kopylov, .M.; Golovin, .V. Classification of G-Quadruplex DN on the Basis of the Quadruplex Twist ngle and Planarity of G-Quartets. *cta Nat.* **2010**, 2, 72–81. [CrossRef]

Disclaimer/Publisher's Note: The statements, opinions and data contained in all publications are solely those of the individual author(s) and contributor(s) and not of MDPI and/or the editor(s). MDPI and/or the editor(s) disclaim responsibility for any injury to people or property resulting from any ideas, methods, instructions or products referred to in the content.